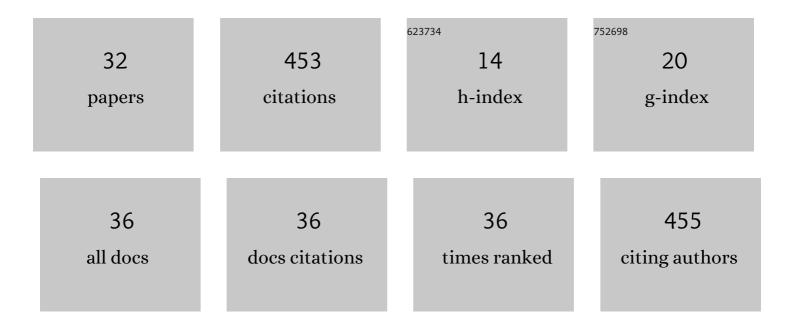
Vasanthan Devaraj

List of Publications by Year in descending order

Source: https://exaly.com/author-pdf/3440085/publications.pdf Version: 2024-02-01



#	Article	IF	CITATIONS
1	Neural mechanism mimetic selective electronic nose based on programmed M13 bacteriophage. Biosensors and Bioelectronics, 2022, 196, 113693.	10.1	18
2	An Accessible Integrated Nanoparticle in a Metallic Hole Structure for Efficient Plasmonic Applications. Materials, 2022, 15, 792.	2.9	7
3	Three-Dimensional Plasmonic Nanocluster-Driven Light–Matter Interaction for Photoluminescence Enhancement and Picomolar-Level Biosensing. Nano Letters, 2022, 22, 4702-4711.	9.1	20
4	Biomaterial actuator of M13 bacteriophage in dynamically tunable plasmonic coupling structure. Sensors and Actuators B: Chemical, 2022, 369, 132326.	7.8	6
5	High quantum efficiency and stability of biohybrid quantum dots nanojunctions in bacteriophage-constructed perovskite. Materials Today Nano, 2021, 13, 100099.	4.6	9
6	Programmable self-assembly of M13 bacteriophage for micro-color pattern with a tunable colorization. RSC Advances, 2021, 11, 32305-32311.	3.6	3
7	Optical bioelectronic nose of outstanding sensitivity and selectivity toward volatile organic compounds implemented with genetically engineered bacteriophage: Integrated study of multi-scale computational prediction and experimental validation. Biosensors and Bioelectronics, 2021, 177, 112979.	10.1	20
8	Engineering Efficient Self-Assembled Plasmonic Nanostructures by Configuring Metallic Nanoparticle's Morphology. International Journal of Molecular Sciences, 2021, 22, 10595.	4.1	8
9	Investigation of colorimetric biosensor array based on programable surface chemistry of M13 bacteriophage towards artificial nose for volatile organic compound detection: From basic properties of the biosensor to practical application. Biosensors and Bioelectronics, 2021, 188, 113339.	10.1	26
10	A DNA-derived phage nose using machine learning and artificial neural processing for diagnosing lung cancer. Biosensors and Bioelectronics, 2021, 194, 113567.	10.1	19
11	Trifluoromethylâ€Group Bearing, Hydrophobic Bulky Cations as Defect Passivators for Highly Efficient, Stable Perovskite Solar Cells. Solar Rrl, 2021, 5, 2100712.	5.8	11
12	A single bottom facet outperforms random multifacets in a nanoparticle-on-metallic-mirror system. Nanoscale, 2020, 12, 22452-22461.	5.6	14
13	Influence of cavity geometry towards plasmonic gap tolerance and respective near-field in nanoparticle-on-mirror. Current Applied Physics, 2020, 20, 1335-1341.	2.4	6
14	Carbon Nanotube Electrodeâ€Based Perovskite–Silicon Tandem Solar Cells. Solar Rrl, 2020, 4, 2000353.	5.8	19
15	Sensitive and label-free shell isolated Ag NPs@Si architecture based SERS active substrate: FDTD analysis and in-situ cellular DNA detection. Applied Surface Science, 2020, 515, 145955.	6.1	17
16	Gap Plasmon of Virusâ€Templated Biohybrid Nanostructures Uplifting the Performance of Organic Optoelectronic Devices. Advanced Optical Materials, 2020, 8, 1902080.	7.3	17
17	Defining the plasmonic cavity performance based on mode transitions to realize highly efficient device design. Materials Advances, 2020, 1, 139-145.	5.4	3
18	Hierarchical Cluster Analysis of Medical Chemicals Detected by a Bacteriophage-Based Colorimetric Sensor Array. Nanomaterials, 2020, 10, 121.	4.1	22

VASANTHAN DEVARAJ

#	Article	IF	CITATIONS
19	Modifying Plasmonic-Field Enhancement and Resonance Characteristics of Spherical Nanoparticles on Metallic Film: Effects of Faceting Spherical Nanoparticle Morphology. Coatings, 2019, 9, 387.	2.6	15
20	Revealing Plasmonic Property Similarities and Differences Between a Nanoparticle on a Metallic Mirror and Free Space Dimer Nanoparticle. Journal of the Korean Physical Society, 2019, 75, 313-318.	0.7	9
21	A facile low-cost paper-based SERS substrate for label-free molecular detection. Sensors and Actuators B: Chemical, 2019, 291, 369-377.	7.8	68
22	Improvement of High Affinity and Selectivity on Biosensors Using Genetically Engineered Phage by Binding Isotherm Screening. Viruses, 2019, 11, 248.	3.3	9
23	Experimental and numerical evaluation of a genetically engineered M13 bacteriophage with high sensitivity and selectivity for 2,4,6-trinitrotoluene. Organic and Biomolecular Chemistry, 2019, 17, 5666-5670.	2.8	8
24	Dependences of the Near-Field Characteristics of the Nano-Gap Structure on the Difference between Pentagonal and Circular Nano-Wires: A Numerical Study. New Physics: Sae Mulli, 2019, 69, 25-30.	0.1	0
25	Numerical Analysis of Nanogap Effects in Metallic Nano-disk and Nano-sphere Dimers: High Near-field Enhancement with Large Gap Sizes. Journal of the Korean Physical Society, 2018, 72, 599-603.	0.7	16
26	Fabrication of Self-Assembled Nanoporous Structures from a Self-Templating M13 Bacteriophage. ACS Applied Nano Materials, 2018, 1, 2851-2857.	5.0	5
27	Deterministic coupling of epitaxial semiconductor quantum dots to hyperbolic metamaterial. Optica, 2018, 5, 832.	9.3	8
28	Self-Assembled Nanoporous Biofilms from Functionalized Nanofibrous M13 Bacteriophage. Viruses, 2018, 10, 322.	3.3	13
29	Distinguishable Plasmonic Nanoparticle and Gap Mode Properties in a Silver Nanoparticle on a Gold Film System Using Three-Dimensional FDTD Simulations. Nanomaterials, 2018, 8, 582.	4.1	32
30	Design for an efficient single photon source based on a single quantum dot embedded in a parabolic solid immersion lens. Optics Express, 2016, 24, 8045.	3.4	16
31	Maximum photon extraction from a single quantum dot embedded in a metal/dielectric-cladded cylindrical structure. Journal of the Korean Physical Society, 2016, 68, 1014-1018.	0.7	3
32	Fabrication of Ultra-smooth 10 nm Silver Films without Wetting Layer. Applied Science and Convergence Technology, 2016, 25, 32-35.	0.9	6